Theory of spin modes in vortex-state ferromagnetic cylindrical dots

R. Zivieri and F. Nizzoli
Dipartimento di Fisica, Università di Ferrara and Istituto Nazionale per la Fisica della Materia, Via Paradiso 12, I-44100 Ferrara, Italy
(Received 8 October 2004; published 7 January 2005)

A theoretical model for the calculation of the quantized spectrum of spin modes frequencies in cylindrical magnetic dots of radius ranging from the nanometric to the submicrometric scale in the vortex ground state at zero applied magnetic field is presented. The effective field includes both the surface and the volume dynamic magnetostatic and exchange fields. We also show that the core energy affects the spin dynamics. The modes at lower frequencies present as radial eigenvectors Bessel functions of high orders ($m \geqslant 1$), while the axially symmetric modes at higher frequencies correspond to zero order Bessel functions.

DOI: 10.1103/PhysRevB.71.014411 PACS number(s): 75.75.+a, 75.30.Ds

I. INTRODUCTION

In the last decade the study of magnetic nanostructures has been of fundamental importance for the numerous applications in the field of high density magnetic storage. Great interest has been also addressed to the experimental study of the spin dynamics of small particles in the vortex state. In particular, a series of recent experimental studies using magneto-optical techniques[1–4] has confirmed the presence of a vortex state in periodic arrays of magnetic dots. Moreover, there is a series of recent measurements performed with magnetic force microscopy,[5] spin polarized scanning tunneling microscopy[6] and x-ray techniques[7] patterns of nano- and micron-sized ferromagnetic dots in the vortex state which have confirmed, as predicted by theory, the formation of a vortex core with the magnetization pointing outside the plane of the dot.

Up to now a general theoretical solution to the problem of spin modes in vortex state ferromagnetic cylindrical dots, free from limiting assumptions, has not yet been reported. Therefore, in this paper we present a complete analytical model for the calculation of the spin modes eigenfrequencies of cylindrical ferromagnetic dots, with aspect ratio $\beta = L/R < 1$ and dot radius R ranging from the nanometric to the submicrometric scale, in the presence of a vortex and for zero external magnetic field. We restrict ourselves to arrays of dots where the interdot distance d is large, so that the interdot magnetostatic energy may be considered negligible. Compared to previous recent approaches,[8,9] we have taken into account in the present model: (a) the core (C) effective field, (b) the dynamic exchange field in the whole dot, (c) both volume and surface dynamic magnetostatic field contributions in the out-of-core (OC) region without any "ultrathin-dot" approximation to obtain the magnetostatic Green's function tensor components, and (d) the dependence of the dynamic magnetization on the z-coordinate perpendicular to the dot plane. The paper is organized as follows. In Sec. II the theoretical model is presented. Section III is devoted to the discussion and to the main numerical results. In Sec. IV the Conclusions are drawn.

II. THEORETICAL MODEL

Under the linear approximation we write the total magnetization as a sum of a static part and a small dynamic part, viz. $\mathbf{M}(\mathbf{r},t) = \mathbf{M}_0 + \mathbf{m}(\mathbf{r},t)$ with $\mathbf{m}(\mathbf{r},t) = \mathbf{m}_0 r(\rho) e^{im\phi} e^{ik_\perp z} e^{-i\omega t}$ in cylindrical coordinates (ρ, ϕ, z); $\mathbf{m}_0$ is the dynamic magnetization amplitude, ω is the spin mode frequency. We assume that $k_\perp \simeq \pm ik$ with $k_\perp$ and k the perpendicular and the in-plane wave vector components, respectively. Due to its angular distribution the "curling" magnetization[10] in the OC region is of the form $\mathbf{M}_0 = (0, M_\phi^{\mathrm{oc}}, 0)$ where ϕ is the azimuthal angle and $|\mathbf{M}_0| = M_s$; instead, in the C region a z-component arises so that $\mathbf{M}_0 = (0, M_\phi^{\mathrm{c}}, M_z)$ becomes perpendicular to the dot surface in the very centre of the dot. The dynamic part of the magnetization is given in the OC region by $\mathbf{m}_{\mathrm{oc}} = (m_\rho, 0, m_z)$ where m_ρ and m_z are the radial and the z-component, respectively. Due to the turning out of the "curling" $\mathbf{M}$, in the C region the precession plane progressively rotates so that $\mathbf{m}_{\mathrm{c}} = (m_\rho, m_{\phi'}, m_{z'})$ with $m_{\phi'} = m_z \cos\theta$ and $m_{z'} = m_z \sin\theta$ where θ is the polar angle between the z-axis and $\mathbf{M}_0$. We decompose the effective field into a static part, $\mathbf{H}_{\mathrm{eff}}(\mathbf{r}) = \mathbf{H}_{\mathrm{eff}}^{\mathrm{oc}}(\mathbf{r}) + \mathbf{H}_{\mathrm{eff}}^{\mathrm{c}}(\mathbf{r})$ including both an OC and a C contribution,[11] and a small dynamic one, $\mathbf{h}_{\mathrm{eff}}(\mathbf{r},t)$, in order to write the linearized equation of motion neglecting the second-order contributions and omitting the spatial and temporal dependences:

$$-\frac{1}{\gamma}\frac{d\mathbf{m}_{\mathrm{oc}}}{dt} = \mathbf{m}_{\mathrm{c}} \times \mathbf{H}_{\mathrm{eff}}^{\mathrm{c}} + \mathbf{m}_{\mathrm{oc}} \times \mathbf{H}_{\mathrm{eff}}^{\mathrm{oc}} + \mathbf{M}_0 \times \mathbf{h}_{\mathrm{eff}}, \qquad (1)$$

where γ is the gyromagnetic ratio. We have made the assumption that $d\mathbf{m}/dt = (1-\eta)(d\mathbf{m}_{\mathrm{oc}}/dt) + \eta(d\mathbf{m}_{\mathrm{c}}/dt) \simeq d\mathbf{m}_{\mathrm{oc}}/dt$, because $d\mathbf{m}_{\mathrm{oc}}/dt \simeq d\mathbf{m}_{\mathrm{c}}/dt$; the term $1-\eta$ with $\eta = a/R$ (a core radius) is a weighting factor for the OC region. The static part of C effective field $\mathbf{H}_{\mathrm{eff}}^{\mathrm{c}}(\mathbf{r}) = \mathbf{H}_{\mathrm{dem}}^{\mathrm{c}}(\mathbf{r}) + \mathbf{H}_{\mathrm{exch}}^{\mathrm{c}}(\mathbf{r}) + \mathbf{H}_{\mathrm{an}}^{\mathrm{c}}(\mathbf{r})$ includes the static exchange, the demagnetizing and the anisotropy C field, respectively. The dynamic part of the effective field is $\mathbf{h}_{\mathrm{eff}}(\mathbf{r},t) = \mathbf{h}_{\mathrm{exch}}(\mathbf{r},t) + \mathbf{h}_{\mathrm{d}}^{\mathrm{oc}}(\mathbf{r},t) + \mathbf{h}_{\mathrm{d}}^{\mathrm{c}}(\mathbf{r},t)$. The nonuniform exchange field in the whole dot is $\mathbf{h}_{\mathrm{exch}}(\mathbf{r},t) = (1-\eta)\mathbf{h}_{\mathrm{exch}}^{\mathrm{oc}}(\mathbf{r},t) + \eta\mathbf{h}_{\mathrm{exch}}^{\mathrm{c}}(\mathbf{r},t)$. Since in principle $\mathbf{h}_{\mathrm{exch}}^{\mathrm{oc}}(\mathbf{r},t) \simeq \mathbf{h}_{\mathrm{exch}}^{\mathrm{c}}(\mathbf{r},t)$ it is also $\mathbf{h}_{\mathrm{exch}}(\mathbf{r},t) \simeq \mathbf{h}_{\mathrm{exch}}^{\mathrm{oc}}(\mathbf{r},t)$. Therefore we may write $\mathbf{h}_{\mathrm{exch}}(\mathbf{r},t) \simeq \alpha\nabla^2\mathbf{m}_{\mathrm{oc}}(\mathbf{r},t)$ where $\alpha = 2A/M_s^2$ is the exchange constant. $\mathbf{h}_{\mathrm{d}}^{\mathrm{oc}}$ and $\mathbf{h}_{\mathrm{d}}^{\mathrm{c}}$ are the OC and C dynamic dipolar field, respectively. Simplifying the time dependence and omitting the

spatial dependence the linearized equations of motion in terms of the OC dynamic magnetization components take the form

$$H_{\mathrm{eff}}^{\mathrm{oc}} m_\rho - M_s h_{d\rho}^{\mathrm{oc}} + H_{\mathrm{exch}}^{\mathrm{c}\phi} m_\rho - M_s h_{d\rho}^{\mathrm{c}} - \alpha M_s \nabla^2 m_\rho = i\Omega m_z, \tag{2}$$

$$H_{\mathrm{eff}}^{\mathrm{oc}} m_z - M_s h_{dz}^{\mathrm{oc}} + H_{\mathrm{exch}}^{\mathrm{c}\phi} m_z \sin\theta - (H_{\mathrm{exch}}^{\mathrm{cz}} + H_{\mathrm{dem}}^{\mathrm{c}} + H_{\mathrm{an}}^{\mathrm{c}}) m_z \cos\theta - M_s h_{dz}^{\mathrm{c}} - \alpha M_s \nabla^2 m_z = -i\Omega m_\rho, \tag{3}$$

where $\Omega = \omega/\gamma$, $H_{\mathrm{exch}}^{\mathrm{c}\phi}$ and $H_{\mathrm{exch}}^{\mathrm{cz}}$ are the ϕ and the z components of the C exchange field averaged over the dot area, respectively. Due to its small effect the contribution of the C $m_{\phi'}$ component to the torque has been neglected. The effective static OC field is composed by both a demagnetizing and an exchange contribution, i.e., $H_{\mathrm{eff}}^{\mathrm{oc}}(\mathbf{r}) = H_{\mathrm{dem}}^{\mathrm{oc}}(\mathbf{r}) + H_{\mathrm{exch}}^{\mathrm{oc}}(\mathbf{r})$. Even if in principle it is locally different from zero and along the direction of the static magnetization, because of the radial symmetry of the vortex state it vanishes if averaged over the ϕ azimuthal coordinate. The OC dynamic dipolar field gives a great contribution to the spin excitations in the presence of a vortex. It may be expressed as a functional of $\mathbf{m}$[12] in terms of the magnetostatic 3×3 tensorial Green's function $\hat{G}$: $\mathbf{h}_{\mathrm{d}}^{\mathrm{oc}}(\mathbf{r}) = (1-\eta)\int_V d^3\mathbf{r}'\hat{G}(\mathbf{r},\mathbf{r}')\mathbf{m}_{\mathrm{oc}}(\mathbf{r}')$ where V is the volume of the OC region. We have calculated the average over the coordinates z and z' $L\langle e^{ik_\perp z} G_{\alpha\beta}(\mathbf{r},\mathbf{r}') e^{ik_\perp z'}\rangle_{z,z'}$ $(\alpha,\beta = \rho, z)$. This average divided by the z component normalization constant turns out to be proportional to the susceptibility fitted by $\chi(kL) = (1-e^{-2kL})/2$. The subsequent ρ' and ϕ' integrations give for the radial component of the $m=0$ modes:

$$h_{\mathrm{d}\rho}^{\mathrm{oc}}(\rho) \simeq -4\pi(1-\eta)\chi(kL) m_\rho(\rho). \tag{4}$$

We have numerically calculated the OC radial component for the $m \neq 0$ modes. The result of the ρ' and ϕ' integrations for the perpendicular component gives instead

$$h_{\mathrm{dz}}^{\mathrm{oc}}(\rho,\phi) \simeq -4\pi(1-\eta)[1-\chi(kL)] m_z(\rho) e^{im\phi}. \tag{5}$$

The quality of the local approximation used in Eq. (4) and Eq. (5) deteriorates when β is near to 1, because the static magnetization at the boundary of the cylinder is then no longer pinned perpendicular to the cylinder axis and can tilt more or less freely in the z direction. The C demagnetizing field $\mathbf{H}_{\mathrm{dem}}^{\mathrm{c}}(\mathbf{r})$ is one order of magnitude smaller than the other two terms of the C static effective field, therefore it has been neglected in the frequency calculation. The largest energy contribution inside the C region comes from the static exchange field $\mathbf{H}_{\mathrm{exch}}^{\mathrm{c}}(\mathbf{r}) = \alpha\nabla^2(0, M_\phi^{\mathrm{c}}, M_z)$. The z component averaged over the dot area $S = \pi R^2$ is

$$H_{\mathrm{exch}}^{\mathrm{cz}} = \pm \frac{\alpha M_s}{S} \int d^2\boldsymbol{\rho} \left[\cos\theta \left(\frac{d\theta}{d\rho}\right)^2 + \sin\theta \frac{d^2\theta}{d\rho^2} + \frac{1}{\rho}\sin\theta\frac{d\theta}{d\rho}\right], \tag{6}$$

where we have taken $M_z^{\mathrm{c}} = \pm M_s \cos\theta(\rho)$[13] with the $+$ $(-)$ indicating that the static magnetization points outward (inward) the dot surface.

In order to carry out explicitly the calculation a form for $\theta(\rho)$ is needed. We assume the Usov distribution,[13] $\theta(\rho) = \arcsin[2a\rho/(a^2+\rho^2)]$ for $\rho \leqslant a$. Substituting it into the integrand $I(\rho)$ of Eq. (6) we get $I(\rho) = 8a^2[(a^2-\rho^2)/(a^2+\rho^2)^3]$. Averaging this expression over S we obtain

$$H_{\mathrm{exch}}^{\mathrm{cz}} = \pm 2\alpha M_s \frac{1}{R^2}. \tag{7}$$

The averaged ϕ component is obtained approximately from the simple relation $H_{\mathrm{exch}}^{\mathrm{c}\phi} = H_{\mathrm{exch}}^{\mathrm{cz}}/\langle\cot\theta\rangle_{\theta(\rho)}$ where $\langle\cdots\rangle_{\theta(\rho)}$ indicates the average of $\cot\theta$ over the $\theta(\rho)$ Usov distribution. The result of this calculation is

$$H_{\mathrm{exch}}^{\mathrm{c}\phi} = 3\alpha M_s \frac{1}{R^2}. \tag{8}$$

Moreover, in the frequency calculation also the uniaxial C anisotropy field $\mathbf{H}_{\mathrm{an}}^{\mathrm{c}}(\mathbf{r})$ has been included. Another non negligible contribution to the spin modes energy arises from the dynamic dipolar field in the C region defined as $\mathbf{h}_{\mathrm{d}}^{\mathrm{c}}(\mathbf{r}) = \eta\int_{V\mathrm{c}} d^3\mathbf{r}' \langle\hat{G}_R(\mathbf{r},\mathbf{r}')\rangle_{\theta(\rho)} \langle\mathbf{m}_{\mathrm{c}}(\mathbf{r}')\rangle_{\theta(\rho)}$ where $\langle\cdots\rangle_{\theta(\rho)}$ indicates the average of the rotated magnetostatic Green's function $\hat{G}_R(\mathbf{r},\mathbf{r}') = \hat{R}^{-1}\hat{G}(\mathbf{r},\mathbf{r}')\hat{R}$ and of the C dynamic magnetization $\mathbf{m}_{\mathrm{c}}$ over the $\theta(\rho)$ Usov distribution in the C region (V_{C} is the C volume); $\hat{R}$ is the rotation matrix defined by the Euler angles $(0, \pi/2-\theta, 0)$. The average over z and z' followed by an integration over ρ' and ϕ' leads for the $m=0$ modes to

$$h_{\mathrm{d}\rho}^{\mathrm{c}}(\rho) \simeq -4\pi\eta\chi(kL) m_\rho(\rho). \tag{9}$$

The C radial component for the $m \neq 0$ modes has been evaluated numerically; instead

$$h_{\mathrm{dz}}^{\mathrm{c}}(\rho,\phi) \simeq -4\pi\eta(4\log 2 - 2)(4-\pi)[1-\chi(kL)] m_z(\rho) e^{im\phi}. \tag{10}$$

The same conclusions concerning the limitations of the local dipolar approximation drawn for the derivation of Eq. (4) and Eq. (5) have to be extended also to Eq. (9) and Eq. (10). Morevover, it is known that the dynamic dipolar field in the C region is not homogeneous along the thickness L if the cylinder becomes sufficiently thick.

We have assumed that, with the previously calculated effective field, the radial parts of Eq. (2) and Eq. (3) allow as solution a combination of two linearly independent Bessel functions of the form $r_m(k\rho) = bJ_m(k\rho) + cY_m(k\rho)$ where the J_m and the Y_m are Bessel functions of order m, of the first and second kind, respectively. We have taken as particular combination of the radial eigenfunctions, for $\rho \gg l_0$ $r_m(k\rho) \propto J_m(k\rho) + \sigma_m(kl_0) Y_m(k\rho)$,[14] where $m = 0, \pm 1, \pm 2\ldots$. $\sigma_m(kl_0)$ is a measure of the scattering of the spin wave modes in the OC region[14] due to the presence of the vortex and l_0 is the reduced exchange length. In principle, in our scheme the scattering amplitude should be derived applying a perturbation approach to Eq. (2) and Eq. (3). However, we have found that the effect of the dipolar term is numerically negligible. Therefore, it is enough to consider the expression of $\sigma_m(kl_0)$ already derived in Ref. 8 and Ref. 15 for an exchange Hamiltonian: $\sigma_{m=0} = (\pi/4)(kl_0)^2 \ln(1/kl_0)$, $\sigma_{m=\mp 1} = \pm(\pi/4)kl_0$ and $\sigma_m \propto (kl_0)^p$ with $p \geqslant 4$ for $|m| > 1$.

Due to the vortex state symmetry we have considered only radial boundary conditions on the lateral dot surface. The quantized wave number κ_{mn} has been obtained as solution of the equation for the m_ρ component of the dynamic magnetization[8] $J'_m(\kappa_{mn}\rho)+\sigma_m(\kappa_{mn}l_0)Y'_m(\kappa_{mn}\rho)+p[J_m(\kappa_{mn}\rho)+\sigma_m(\kappa_{mn}l_0)Y_m(\kappa_{mn}\rho)]=0$ with p the pinning parameter given in Ref. 8 and n the number of nodes in the half dot ($n=0,1,\cdots$). We have also supposed the m_z component with the same quantization condition as m_ρ. From Eq. (2) and Eq. (3) and from the radial boundary condition, an analytical expression for the quantized spectrum of the vortex spin modes can be obtained. One first multiplies Eq. (2) and Eq. (3) together; multiplying the result of this operation on the left by m_ρ^* and by m_z^*, assuming the dynamic exchange field uniform along the thickness L, integrating over $d^2\boldsymbol{\rho}$, and finally dividing by the in-plane normalization constant N it can be shown that the diagonal spectrum is given by

$$\begin{aligned}\Omega_{mn}^2 = \Omega_M^2\big[&\xi(\kappa_{mn}L)^2+3\xi+\chi(\kappa_{mn}L)c_m\big]\\ &\times\big[\xi(\kappa_{mn}L)^2+\mathrm{k_{an}}[1-(3-4\log 2)\eta^2]\\ &+3\xi(4-\pi)-2\xi(2\log 2-1)\\ &+[1-\chi(\kappa_{mn}L)][(1-\eta)+\eta(4-\pi)(4\log 2-2)]\big].\end{aligned} \tag{11}$$

$\Omega_M=4\pi M_0$, $\mathrm{k_{an}}=8\pi K_1/\Omega_M^2$ is the reduced anisotropy field constant and $\xi=\alpha/4\pi R^2$; n is the number of radial nodes in the half dot. We have calculated c_m for $m=0-4$ finding $c_0=1$ for each n and $c_1=0.40$, $c_2=0.27$, $c_3=0.21$, and $c_4=0.15$ for $n=0$.

III. DISCUSSION AND RESULTS

Numerical calculations have been performed for Permalloy (Py) which presents a "curling" magnetization using material parameters of the continuous film:[16] $4\pi M_S=9.5$ kOe, $\gamma/2\pi=2.996$ GHz/kOe, $\alpha/4\pi=2.42\times10^{-13}$ cm^2; in addition we have taken $K_1=0$. Since the rigid vortex model underestimates the C radius especially at small L, we have taken $a=26$ nm for the range of thicknesses investigated (as can be determined by the micromagnetic approach[17]). The results for the calculated frequency of selected spin modes [from Eq. (11)] are given in Fig. 1, as a function of the dot radius R, in the case of thickness $L=50$ nm. The main findings are the general decrease of the mode frequency versus R (due to a reduction of the dynamic exchange field) and the fact that the frequencies of the axially symmetric modes $(0,n)$ are higher than those of the $(|m|,n)$ modes with $m\neq0$, at least for $n=0$. This behavior may be explained in terms of the larger contribution of the volume dynamic dipolar field to the spin dynamics of the $m=0$ modes with respect to the modes of higher order m. While the decrease of the mode frequency versus R was also found by Ivanov and Zaspel,[8] these authors found a different behavior of the mode frequency with respect to the mode indices m and n. In particular in Ref. 8 a general monotonic increase of the frequency versus m (at fixed n) has been obtained, with the important exception of the $m=\pm1$ modes whose very soft frequency (less than 1 GHz) was attributed to their nature of vortex translational modes. No mode in this frequency range was found in our framework (see discussion about Fig. 2). While the general behavior of the modes shown in Fig. 1 (with respect to the mode index m) is different from that of Ivanov and Zaspel,[8] it is similar to that provided by a numerical calculation[18] based on a recently proposed "dynamical matrix" micromagnetic approach.[19] Indeed, in Ref. 8 no volume dynamic dipolar terms are included in the effective field and the dynamic exchange contribution is treated in the

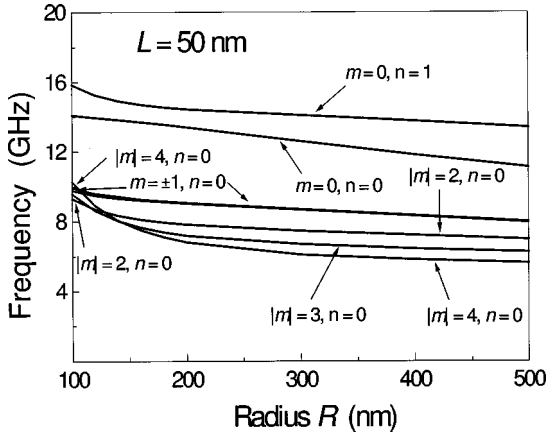

FIG. 1. Frequencies of the $(0,n)$ with $n=0,1$ compared to that of the $(|m|,n)$, with $n=0$ as a function of R. $|m|$ labels the $\pm m$ modes.

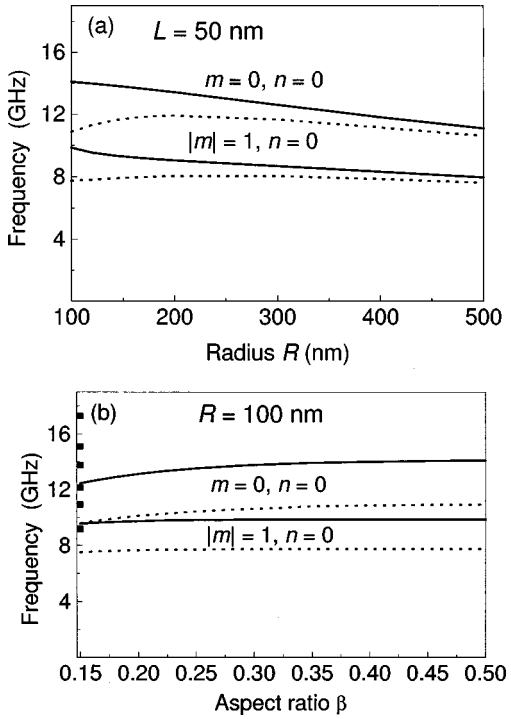

FIG. 2. Panel (a): Frequency of the $m=0$, $n=0$ and of the $|m|=1$, $n=0$ modes. Full lines: calculated frequencies using Eq. (11). Dotted lines: calculated frequencies neglecting the C field. Panel (b): As in panel (a), but as a function of the aspect ratio β for $R=100$ nm. Full squares: Brillouin light scattering experimental frequencies (from Ref. 18).

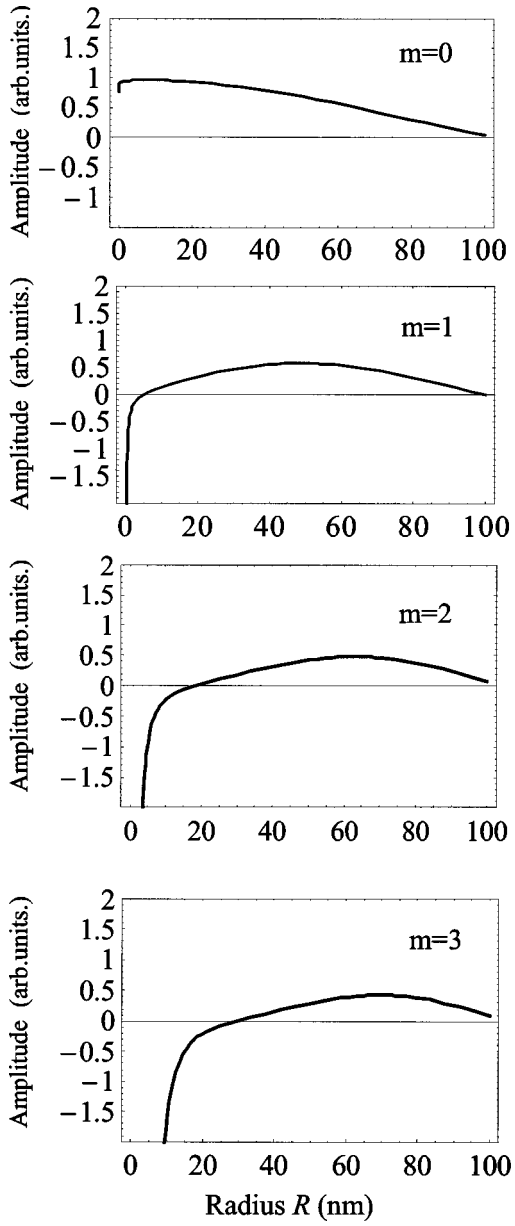

FIG. 3. Radial part of the m_ρ component for the modes with $m=0,1,2,3$ calculated for a dot with $R=100$ nm and $L=15$ nm.

framework of the long-wave approximation which gives a frequency linearly proportional to the wave vector k. The $(|m|,0)$ family of modes presents a frequency spread for each R. Moreover, by increasing R the dynamic exchange field becomes less important, with respect to the corresponding h_{dz} component of the dynamic dipolar field. Finally, for $R=100$ nm the splitting of the $|m|=1$ modes due to the presence of the C is about 0.3 GHz. It becomes negligible for larger R and higher order modes; this result is very similar to that predicted in Ref. 8.

The behavior of the two relevant modes ($m=0,n=0$, the "fundamental mode" of the system) and $(|m|=1,n=0)$ is studied in Fig. 2 as a function of R (for fixed thickness $L=50$ nm) and β (for fixed radius $R=100$ nm). The dotted lines represent the frequencies of the above modes calculated according to Eq. (11), but without the C field, i.e., neglecting

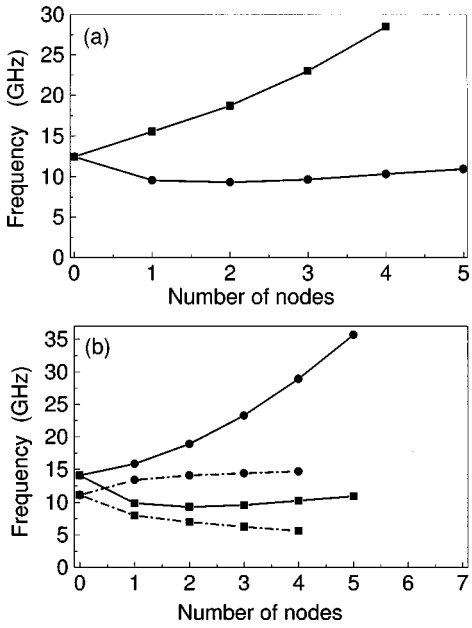

FIG. 4. Frequency dispersion as a function of the number of nodes of the m_ρ component. The lines connecting the points are guides to eye. Panel (a): Calculations at $R=100$ nm and $L=15$ nm. Full squares: $(0,n)$ modes. Full circles: $(|m|,0)$ modes. Panel(b): Full line: calculations at $R=100$ nm and $L=50$ nm. Dash-dotted line: calculations at $R=500$ nm and $L=50$ nm. The meaning of the symbols is reversed compared to panel (a).

the contributions of the C fields given in Eqs. (7)–(10) together with the numerically calculated C radial component of the $m\neq 0$ modes dynamic dipolar field. The effect of the C field on the $m=0$, $n=0$ mode frequency is about 30% for $R=100$ nm and only 5% for $R=500$ nm. This smaller effect with increasing R is due to a decreasing of the C effective field in dots of large radius. The C field also affects the dynamics of the $|m|=1$ mode (as well as that of higher order modes) in the whole range of radii investigated, increasing the frequency of more than 25% at small R. The calculated frequency as a function of β is shown in panel (b) of Fig. 2 and is compared with the experimental frequencies measured by Brillouin light scattering technique for $\beta=0.15$.[18] The agreement between the measured and the calculated frequencies for the $|m|=1$, $n=0$ and $m=0$, $n=0$ modes is very good provided that the effect of the C field is included.

As far as the pinning of the modes is concerned, we have found that for small dot radius the modes with $m\leqslant 1$ are pinned at the dot boundary while the pinning decreases with increasing the mode order m. This is shown in Fig. 3 for the case $R=100$ nm and $L=15$ nm. The same effect is also present at larger R, but it occurs at higher mode order. A similar behavior has been reported by Guslienko *et al.*[20] for the modes magnetization profiles in thin magnetic stripes. In both approaches the pinning parameter depends on the geometry of the magnetic element, but from the boundary condition it results that only in the present study the pinning decreases with increasing the mode number m. However, in the case of magnetic stripes the pinning parameter is of purely dipolar nature and decreases with increasing the width stripe at fixed thickness, whereas in the present study it ex-

presses the competition between the dipolar and the exchange energy at the boundary and increases with increasing R. It is important to underline that magnetic stripes studied in Ref. 20 are in a saturated state, while cylindrical dots of the present study are in a vortex state.

In Fig. 4 the frequency vs the number of nodes for both $(0,n)$ and $(|m|,n)$ modes is shown. In panel (a) we report on the results of the calculations for $R=100$ nm and $L=15$ nm. One notes the similarity of the upper branch (full circles) with the behavior of the Damon-Eshbach-like modes of the saturated state, i.e. the frequency increases with the number of nodes. Conversely, due to competition between the exchange and the dipolar terms, the modes of the lower branch show an initial decrease of the frequency with a minimum for $m=2$, followed by a successive increase, analogously to the backwardlike modes of the saturated state.[16] In panel (b) are shown the results of the calculations at $L=50$ nm and for $R=100$ nm and $R=500$ nm. Due to a reduction of the dynamic exchange at $R=500$ nm (dash-dotted lines in Fig. 4) the frequency increase of the $(0,n)$ modes is less pronounced with respect to that of the $R=100$ nm dots. Moreover, the minimum in the frequency dispersion of the $(|m|,n)$ modes is at $m=2$ for $R=100$ nm.

IV. CONCLUSIONS

In conclusion, we have investigated the spin excitations of a cylindrical dot in presence of a vortex including in the effective field a full dependence from the dynamic exchange and dipolar contributions. We have also shown the role played by the exchange core energy in the spin excitations, especially for small radii. The introduction of the z-dependence in the dynamic magnetization profile has allowed us to investigate also dots of moderate aspect ratio $(\beta<1)$.

ACKNOWLEDGMENTS

Work supported by Ministero Istruzione, Università e Ricerca through Grant No. PRIN 2003025857 and FIRB Project No. RBNE017XSW. The authors acknowledge G. Gubbiotti and G. Carlotti for the permission to reproduce Brillouin Light Scattering data prior to publication.

[1] R. P. Cowburn, D. K. Koltsov, A. O. Adeyeye, M. E. Welland, and D. M. Tricker, Phys. Rev. Lett. **83**, 1042 (1999).
[2] C. A. Ross, M. Hwang, M. Shima, J. Y. Cheng, M. Farhoud, T. A. Savas, Henry I. Smith, W. Schwarzacher, F. M. Ross, M. Redjdal, and F. B. Humphrey, Phys. Rev. B **65**, 144417 (2002).
[3] V. Novosad, K. Yu. Guslienko, H. Shima, Y. Otani, S. G. Kim, K. Fukamichi, N. Kikuchi, O. Kitakami, and Y. Shimada, Phys. Rev. B **65**, 060402(R) (2002).
[4] M. Grimsditch, P. Vavassori, V. Novosad, V. Metlushko, H. Shima, Y. Otani, and K. Fukamichi, Phys. Rev. B **65**, 172419 (2002).
[5] T. Shinjo, T. Okuno, R. Hassdorf, K. Shigeto, and T. Ono, Science **289**, 5481 (2000).
[6] A. Wachowiak, J. Wiebe, M. Bode, O. Pietzsch, M. Morgenstern, and R. Wiesendanger, Science **298**, 577 (2002).
[7] S.-B. Choe, Y. Acremann, A. Scholl, A. Bauer, A. Doran, J. Stöhr, and H. A. Padmore, Science **304**, 420 (2004).
[8] B. A. Ivanov and C. E. Zaspel, Appl. Phys. Lett. **81**, 1261 (2002).
[9] V. Novosad, M. Grimsditch, K. Yu. Guslienko, P. Vavassori, Y. Otani, and S. D. Bader, Phys. Rev. B **66**, 052407 (2002).
[10] A. Aharoni, J. Appl. Phys. **68**, 2892 (1990).
[11] N. A. Usov and S. E. Peschany, Fiz. Met. Metalloved. **78**, 13 (1994) (in Russian).
[12] K. Yu. Guslienko and A. N. Slavin, J. Appl. Phys. **87**, 6337 (2000).
[13] N. A. Usov and S. E. Peschany, J. Magn. Magn. Mater. **118**, L290 (1993).
[14] B. A. Ivanov, H. J. Schnizer, F. G. Mertens, and G. M. Wjsin, Phys. Rev. B **58**, 8464 (1998).
[15] B. A. Ivanov and I. A. Yastremskii, Low Temp. Phys. **26**, 341 (2000).
[16] G. Gubbiotti, G. Carlotti, T. Okuno, T. Shinjo, F. Nizzoli, and R. Zivieri, Phys. Rev. B **68**, 184409 (2003).
[17] M. J. Donahue and D. G. Porter, OOMMF User's Guide, NIST, Gaithersburg, MD.
[18] L. Giovannini, F. Montoncello, F. Nizzoli, G. Gubbiotti, G. Carlotti, T. Okuno, T. Shinjo, and M. Grimsditch, Phys. Rev. B **70**, 172404 (2004).
[19] M. Grimsditch, L. Giovannini, F. Montoncello, F. Nizzoli, Gary K. Leaf, and Hans. G. Kaper, Phys. Rev. B **70**, 054409 (2004).
[20] K. Yu. Guslienko, S. O. Demokritov, B. Hillebrands, and A. N. Slavin, Phys. Rev. B **66**, 132402 (2002).